

# Modulation of Stacking Interactions by Transition-Metal Coordination: Ab Initio Benchmark Studies

Shaun T. Mutter and James A. Platts\*[a]

**Abstract:** A series of ab initio calculations are used to determine the C–H $\cdots\pi$  and  $\pi\cdots\pi$ -stacking interactions of aromatic rings coordinated to transition-metal centres. Two model complexes have been employed, namely, ferrocene and chromium benzene tricarbonyl. Benchmark data obtained from extrapolation of MP2 energies to the basis set limit, coupled with CCSD(T) correction, indicate that co-ordinated aromatic rings are slightly

weaker hydrogen-bond acceptors but are significantly stronger hydrogen-bond donors than uncomplexed rings. It is found that  $\pi\cdots\pi$  stacking to a second benzene is stronger than in the free benzene dimer, especially in the

**Keywords:** ab initio calculations • hydrogen bonds • metallocenes • stacking interactions • transition metals

chromium case. This is assigned, by use of energy partitioning in the local correlation method, to dispersion interactions between metal d and benzene  $\pi$  orbitals. The benchmark data is also used to test the performance of more efficient theoretical methods, indicating that spin-component scaling of MP2 energies performs well in all cases, whereas various density functionals describe some complexes well, but others with errors of more than 1 kcal mol<sup>-1</sup>.

## Introduction

The intermolecular interactions of aromatic molecules are of great interest across chemistry, biology and materials science. Specifically, hydrogen bonds in which aromatic molecules act as donors and/or acceptors are increasingly recognised as playing an important role in molecular recognition.<sup>[1]</sup> Face-to-face  $\pi$ -stacking interactions, driven largely by dispersion forces, rival hydrogen bonds for stability,<sup>[2]</sup> and are vital in determining the structure and properties of biological molecules such as proteins and nucleic acids.

The archetypal models of such interactions employ the simplest aromatic molecule, benzene, and its dimers and complexes with other small molecules. The complex formed between benzene and methane, for example, is bound by a C–H $\cdots\pi$  hydrogen bond,<sup>[3]</sup> as is the T-shaped dimer of benzene.<sup>[4]</sup> The face-to-face,  $\pi$ -stacked form of the benzene dimer has comparable energy to that of the T-shaped form, with a minimum energy geometry in the off-centre parallel-displaced (PD;  $C_{2h}$ ) rather than the higher symmetry sandwich ( $D_{6h}$ ) form.<sup>[5]</sup>

Experimental data on such systems is hard to come by, and environmental effects such as solvation can be difficult to separate from the inherent effects of the interactions of interest, so theoretical studies of model complexes are crucial in gaining a deeper understanding. However, many approximate methods fail to give even a qualitatively correct description, and high-level ab initio methods are required to achieve acceptable accuracy. This is primarily due to the importance of dispersion forces in determining interaction energies, which in turn means that electron correlation must be taken into account. The simplest approach to this, second-order Møller-Plesset (MP2), is known to overestimate the strength of dispersion interactions by as much as 100%.<sup>[6]</sup> The currently accepted standard approach involves extrapolation of MP2 correlation energies to the basis set limit, along with correction for the shortcomings of MP2 by use of CCSD(T) calculations in smaller basis sets. The resulting predictions, termed CBS(T), are believed to be within a small fraction of 1 kcal mol<sup>-1</sup> of true interaction energies.<sup>[5,7]</sup>

In contrast, many standard methods of quantum chemistry give quantitatively incorrect descriptions of C–H $\cdots\pi$  or  $\pi$ -stacking interactions. Hartree-Fock (HF) methods fail to give any stabilisation whatsoever, due to lack of dispersion by construction. Most DFT methods also fail to properly describe dispersion interactions,<sup>[8]</sup> although recent studies indicate some functionals that do perform well.<sup>[9]</sup> Significant

[a] S. T. Mutter, J. A. Platts  
School of Chemistry, Cardiff University  
Park Place, Cardiff CF10 3AT (UK)  
Fax: (+44) 2920-874030  
E-mail: platts@cf.ac.uk

recent efforts have also been focussed on complementing DFT calculations with empirical dispersion corrections, with impressive results.<sup>[10]</sup> Recent developments indicate that methods such as spin-component scaling,<sup>[11]</sup> quantum Monte Carlo<sup>[12]</sup> and explicit correlation (F12)<sup>[13]</sup> methods are all suitable for describing non-covalent interactions. However, CBS(T) data are still the benchmark against which others methods are tested.

Thus, accurate theoretical studies of model systems give valuable insight into the origin, strength and geometry of these important interactions. However, such methods have not, to date, been applied to systems in which aromatic rings act as ligands to transition metals. This is of more than just academic interest; metal–arene complexes are common in catalysis,<sup>[14]</sup> chemical sensors<sup>[15]</sup> and bio-inorganic chemistry.<sup>[16]</sup> For example, our interest in this field was prompted by the elegant ruthenium–arene complexes designed as anticancer drugs by Sadler et al.<sup>[17]</sup> In these, the coordinated arene is designed to coordinate through stacking and/or C–H... $\pi$  interactions to DNA, thus distorting the double-helix structure and ultimately leading to programmed cell death, or apoptosis. However, little or no information is available on the effect of ruthenium coordination on the interactions of aromatic ligands, or on appropriate theoretical methods for description of such interactions.

In this work, we have employed modern ab initio methods to determine the strength and preferred geometry of intermolecular interactions in two model metal–arene complexes. We have also used this data to benchmark more approximate ab initio and DFT methods that should prove useful in studying larger, more realistic systems. Figure 1 shows schematic representations of the complexes considered.

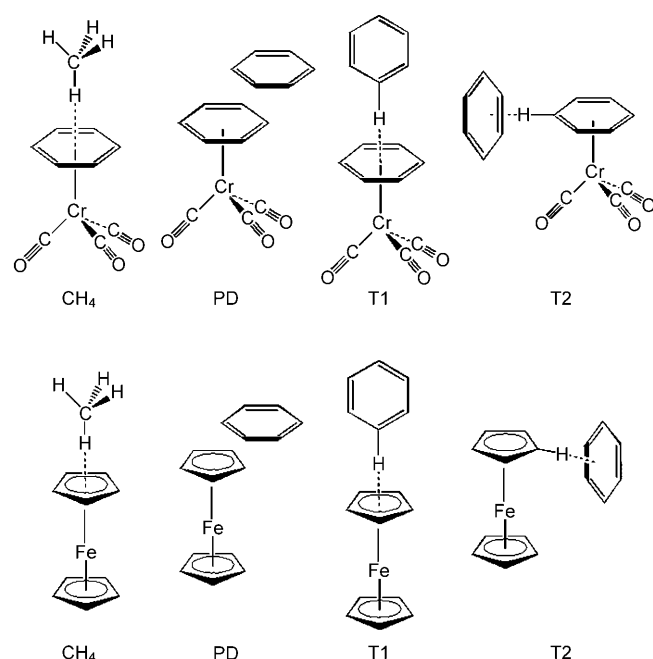


Figure 1. Schematic representation of the complexes considered.

## Computational Methods

All ab initio calculations were performed by using the Molpro suite of programs<sup>[18]</sup> that employed correlation-consistent basis sets.<sup>[19]</sup> Typically, augmented sets aug-cc-pVnZ were used on heavy atoms and non-augmented sets cc-pVnZ were used on hydrogen. This removal of diffuse functions from hydrogen, denoted AVnZ\*, has been shown to significantly reduce calculation times and basis set superposition error (BSSE) with little loss of accuracy in interaction energies. All MP2 calculations employed the density fitting (DF) approximation for calculation of both underlying HF and correlation energy,<sup>[20]</sup> with the aug-cc-pVTZ fitting basis sets for HF and MP2 employed where available,<sup>[21]</sup> and the def2-QZVPP JK-fitting basis on Cr and Fe for DF-HF calculations.<sup>[22]</sup>

CBS(T) data were obtained from extrapolation of DF-MP2 energies with AVDZ\* and AVTZ\* by using the  $E_n^{\text{CORR}} = E_n^{\text{CBS}} + Bn^{-3}$  formula of Helgaker et al.<sup>[23]</sup> The MP2 basis set limit that was found was then corrected for the known shortcomings of MP2 by applying a  $\Delta\text{CCSD(T)}$  correction, that is, the difference in correlation energy between MP2 and CCSD(T), obtained with cc-pVDZ.<sup>[19]</sup> All such data were corrected for BSSE by using the counterpoise method.<sup>[24]</sup> No account was made in such ab initio calculations for relaxation energy between interacting and non-interacting isolated system geometries, that is, intermolecular complexes were constructed from monomers at their equilibrium geometries.

We have also carried out MP2 calculations within the local correlation approach, exploiting the short-range nature of electron correlation, which decays as  $r^{-6}$ .<sup>[25]</sup> After localisation of the canonical HF orbitals, only excitations to virtual orbitals that are spatially close are considered. Coupled with DF methods, this approach can lead to significant savings in computational resources, and can approach linear scaling with system size in favourable cases.<sup>[20]</sup> This DF-LMP2 method, coupled with AVTZ\*, was successfully applied to the various forms of the benzene dimer recently,<sup>[26]</sup> and also effectively eliminates BSSE and the need for counterpoise correction. The localised orbitals required for DF-LMP2 were generated through the Pipek-Mezey method,<sup>[27]</sup> whereas the orbital domain selection followed the procedure of Boughton and Pulay,<sup>[28]</sup> with merging of rotationally invariant  $\pi$  domains where appropriate. All domains were calculated with a large intermolecular separation and then fixed for calculations on the interacting system. The use of localised orbitals also allows decomposition of total correlation energies into intra- and intermolecular contributions, and even from interactions between specific orbitals on separate molecules, as set out by Schütz.<sup>[29]</sup>

Associated with these DF-LMP2 methods, spin-component scaling (SCS) has been used to correct the known shortcomings of MP2-based data at no extra computational cost. This approach separately scales the correlation energy due to parallel and anti-parallel spin electron pairs. In its original form proposed by Grimme, the scaling parameters were optimised to improve on MP2 for a wide range of thermodynamic, kinetic and geometrical properties.<sup>[30]</sup> Three further variants of SCS have been employed, all specifically optimised for description of non-covalent interactions. The first, termed SCSN, uses new scaling parameters to improve DF-LMP2/AVTZ\* prediction of binding energy for stacked nucleic acid base pairs.<sup>[31]</sup> The second, termed SCS(MI), also uses modified scaling parameters, but is based on MP2 correlation energies extrapolated to the basis set limit.<sup>[32]</sup> Both methods result in errors of around 0.3 kcal mol<sup>-1</sup> compared to CBS(T) data over a representative set of intermolecular interactions. The third method, termed SCSC, was optimised for study of catalysis and included total energies as well as interaction energies.<sup>[33]</sup>

DFT calculations were performed by using Gaussian 09,<sup>[34]</sup> using the 6-31+G(d,p) basis set.<sup>[35]</sup> Initial optimisations were performed with the BP86 functional,<sup>[36]</sup> which is widely used in description of organometallic complexes. Two functionals that show promise for description of intermolecular interactions were employed, namely, Becke's half-and-half method, BHandH, and Truhlar's M06-2X and M06-2X functionals.<sup>[9]</sup> The former performs surprisingly well for stacking interactions, apparently through error cancellation, whereas the latter were specifically designed to correct for the shortcomings of traditional DFT methods in describing non-covalent interactions. All DFT interaction energies were corrected

for BSSE by using the counterpoise method.<sup>[24]</sup> Natural bond orbital (NBO) analysis was performed with the NBO 5.G program.<sup>[37]</sup>

## Results and Discussion

The geometries of  $\text{Cr}(\text{C}_6\text{H}_6)(\text{CO})_3$  and  $\text{Fe}(\text{C}_5\text{H}_5)_2$  were optimised without symmetry restrictions by using BP86/6-31+G(d,p), and the resulting structures were confirmed as a true minima through harmonic frequency calculation. Both are in excellent agreement with available experimental data, taken from low-temperature X-ray<sup>[38]</sup> and gas-phase electron diffraction studies,<sup>[39]</sup> respectively, as outlined in Table 1.

Table 1. Comparison of experimental and optimised geometries for  $\text{Cr}(\text{C}_6\text{H}_6)(\text{CO})_3$  and  $\text{Fe}(\text{C}_5\text{H}_5)_2$  [ $\text{\AA}$ ], [ $^\circ$ ].

	Exptl [a]	DFT
$\text{Cr}(\text{C}_6\text{H}_6)(\text{CO})_3$		
Cr–C	1.834 (4)	1.839
C–O	1.173 (9)	1.174
Cr–C	2.233 (9)	2.229
C–C	1.414 (9)	1.426
$\text{Fe}(\text{C}_5\text{H}_5)_2$		
Fe–C	2.054 (3)	2.047
C–C	1.435 (2)	1.441
C–H	1.080 (7)	1.091
mean–C–H <sup>[b]</sup>	3.7 (9)	1.35

[a] Estimated standard deviations given in parenthesis. [b] Angle between C–H and the mean plane of C.

Complexes of  $\text{Cr}(\text{C}_6\text{H}_6)(\text{CO})_3$  and  $\text{Fe}(\text{C}_5\text{H}_5)_2$  with methane, with one C–H bond of the latter directed toward the centroid of the aromatic ligand, were constructed, and rigid scans of the H...arene distances were performed by using DF-LMP2/AVTZ\*. The results of these scans are shown in Figure 2 (HF interaction energies are uniformly positive, and so are not shown here). Both plots are similar in overall form, and it is evident that DF-LMP2 and the two variants of SCS agree on the general features of these complexes, with stabilisation relative to separate monomers for separations of over 2.3 to 2.4  $\text{\AA}$ , and minima at approximately 2.8  $\text{\AA}$ . As has been observed in previous studies, SCSN is bracketed by DF-LMP2 and SCS interaction energies, typical of the tendency of the former to overestimate and the latter to underestimate interaction energies of such non-covalent interactions.

The methods used in Figure 2 have been extensively tested on small, organic model systems, but are as yet untried for the intermolecular interactions of transition-metal complexes. We have, therefore, calculated CBS(T) interaction energies at the separations corresponding to minima of the SCSN curves. The resulting data, along with results from more approximate methods, is presented in Table 2. Our best estimates of interaction energies are  $-1.27 \text{ kcal mol}^{-1}$  and  $-1.47 \text{ kcal mol}^{-1}$ , for the Cr and Fe complexes, respectively, which differ only very slightly from the value of  $-1.45 \text{ kcal mol}^{-1}$  for benzene...methane calculated by using

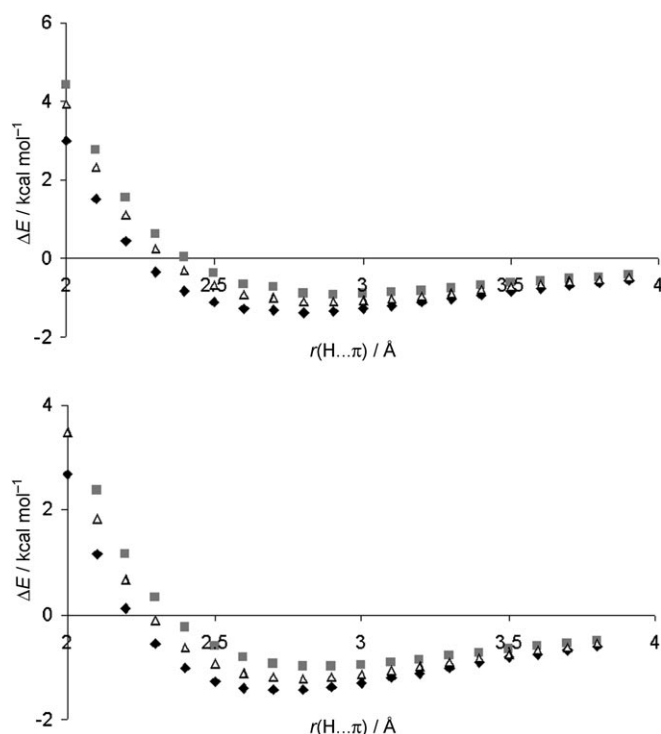


Figure 2. Scans of  $\text{Cr}(\text{C}_6\text{H}_6)(\text{CO})_3$  and  $\text{Fe}(\text{C}_5\text{H}_5)_2$  with  $\text{CH}_4$  ( $\blacklozenge$  = DF-LMP2,  $\blacksquare$  = SCS and  $\triangle$  = SCSN).

similar methods.<sup>[3]</sup> These data also suggest that ferrocene is a slightly better hydrogen-bond acceptor than  $\text{Cr}(\text{C}_6\text{H}_6)(\text{CO})_3$ . The MP2 values are close to the CBS(T) data, and increase with basis set size to values 0.15–0.20  $\text{kcal mol}^{-1}$  greater than the CBS(T) value, indicating that the correction from MP2 to CCSD(T) is small. The perturbative triples contribution is small but important, because neglecting this term and using  $\Delta\text{CCSD}$  only leads to significant over-correction from MP2 data.

The DF-LMP2 interaction energies with AVTZ\* (without counterpoise correction) are close to the corrected, conventional DF-MP2 value, illustrating the essentially BSSE-free nature of this approach. The basis effect in these complexes is rather small, with interaction energies increasing by less than 0.2  $\text{kcal mol}^{-1}$  from AVDZ\* to AVTZ\*. The SCS interaction energy is rather too low, but SCSN performs better and is as close to the CBS(T) value as the MP2 basis set limit, and performance of SCS(MI) and SCSC is similar to SCSN. As expected, HF provides no stabilisation due to the importance of dispersion forces. In contrast, all three DFT methods give reasonable estimates of interaction energies: the values from BHandH are fortuitously close to the best estimate, given that the average error over a set of 22 complexes of small molecules was over 2  $\text{kcal mol}^{-1}$ .<sup>[9]</sup>

Analogous scans were performed for the PD complexes of benzene with  $\text{Cr}(\text{C}_6\text{H}_6)(\text{CO})_3$  and  $\text{Fe}(\text{C}_5\text{H}_5)_2$ , in which benzene was placed at an offset equal to 1.6  $\text{\AA}$ , the optimal value in the isolated benzene dimer. Figure 3 shows interac-

Table 2. Interaction energies for  $\text{Cr}(\text{C}_6\text{H}_6)(\text{CO})_3$  and  $\text{Fe}(\text{C}_5\text{H}_5)_2$  with  $\text{CH}_4$  and  $\text{C}_6\text{H}_6$  [ $\text{kcal mol}^{-1}$ ].<sup>[a]</sup>

	$\text{CH}_4$	PD	T1	T2b
$\text{Cr}(\text{C}_6\text{H}_6)(\text{CO})_3$				
CBS(T) <sup>[b]</sup>	−1.27	−4.22	−2.38	−5.85
MP2/CBS+ $\Delta\text{CCSD}$	−1.11	−3.36	−1.93	−5.15
DF-HF/AVTZ*	+0.59	+3.11	+1.88	+0.70
DF-MP2/AVDZ*	−1.21	−5.47	−2.48	−6.15
DF-MP2/AVTZ*	−1.34	−5.82	−2.75	−6.72
MP2/CBS	−1.46	−6.11	−3.01	−7.26
DF-LMP2/AVTZ*	−1.35	−5.62	−2.53	−6.49
SCS <sup>[c]</sup>	−0.92	−3.76	−1.53	−4.74
SCSN <sup>[c]</sup>	−1.11	−4.35	−2.03	−5.89
SCS(MI) <sup>[c]</sup>	−1.05	−4.18	−1.94	−5.53
SCSC <sup>[c]</sup>	−1.29	−5.44	−2.38	−6.14
BHandH/6-31+G(d,p)	−1.29	−2.92	−2.06	−6.12
M05-2X/6-31+G(d,p)	−0.85	−2.23	−1.15	−4.25
M06-2X/6-31+G(d,p)	−0.90	−3.19	−1.51	−4.69
	$\text{CH}_4$	PD	T1	T2
$\text{Fe}(\text{C}_5\text{H}_5)_2$				
CBS(T) <sup>[b]</sup>	−1.47	−3.00	−2.86	−3.57
MP2/CBS+ $\Delta\text{CCSD}$	−1.31	−2.27	−2.47	−3.03
DF-HF/AVTZ*	+0.42	+3.68	+0.73	+1.75
DF-MP2/AVDZ*	−1.28	−3.84	−2.80	−3.72
DF-MP2/AVTZ*	−1.46	−4.10	−3.08	−4.08
MP2/CBS	−1.63	−4.29	−3.37	−4.40
DF-LMP2/AVTZ*	−1.44	−3.99	−2.97	−3.94
SCS <sup>[c]</sup>	−0.99	−2.44	−2.08	−2.66
SCSN <sup>[c]</sup>	−1.23	−2.71	−2.65	−3.28
SCS(MI) <sup>[c]</sup>	−1.16	−2.64	−2.47	−3.09
SCSC <sup>[c]</sup>	−1.36	−3.91	−2.79	−3.75
BHandH/6-31+G(d,p)	−1.69	−1.60	−2.95	−3.17
M05-2X/6-31+G(d,p)	−1.05	−1.01	−1.92	−2.05
M06-2X/6-31+G(d,p)	−1.16	−1.90	−2.19	−2.42

[a] All data except those based on DF-LMP2 are counterpoise corrected.

[b] Equivalent to MP2/CBS+ $\Delta\text{CCSD}$ (T). [c] See the text for definitions.

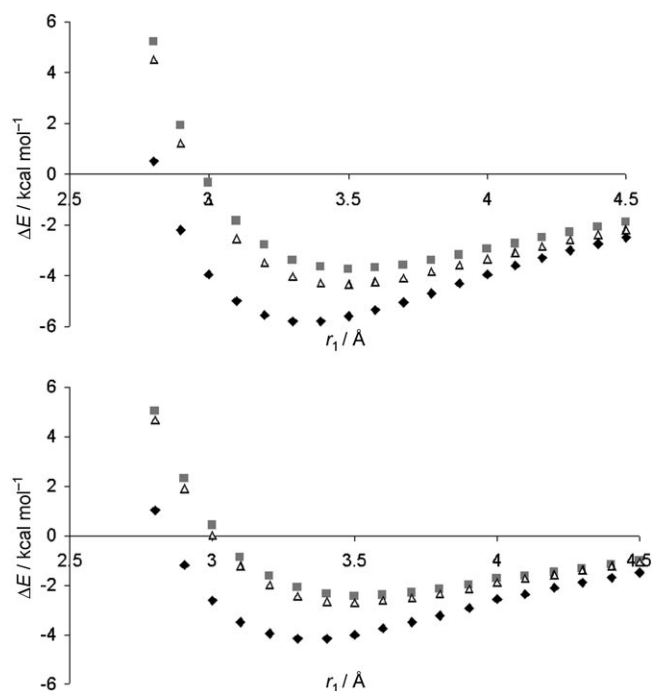


Figure 3. Scan of the PD complex of  $\text{Cr}(\text{C}_6\text{H}_6)(\text{CO})_3$  and  $\text{Fe}(\text{C}_5\text{H}_5)_2$  with  $\text{C}_6\text{H}_6$  (◆ = DF-LMP2, ■ = SCS and △ = SCSN).

tion energies as a function of vertical separation,  $r_1$ , obtained from DF-LMP2/AVTZ\* calculations. In the benzene dimer, DF-LMP2 strongly overestimates interaction energies, so we surmise that the large interaction energies seen in Figure 3 are also overestimates. The SCS values are much smaller, and the SCSN curves are close to the SCS curves, both becoming negative around 3 Å and reaching minima at approximately 3.5 Å. Once again HF data are positive everywhere, and are, therefore, not shown. A scan of horizontal displacement, or offset, (also not shown) by using DF-LMP2/AVTZ\* indicates a shallow minimum around 1.5 Å, with the sandwich structure ( $r_2=0$ ) approximately 1  $\text{kcal mol}^{-1}$  less stable than the PD one.

Table 2 also reports CBS(T) data and approximations to this for the minima of the SCSN curves. For the chromium complex, the CBS(T) value of  $-4.22 \text{ kcal mol}^{-1}$  is significantly more negative than the analogous value for the PD benzene dimer ( $-2.63 \text{ kcal mol}^{-1}$ ). This is something of a surprise, because one might expect the  $\pi$  electrons in free benzene to be less-tightly bound, and hence more polarisable and able to interact through dispersion, than those in benzene that is  $\eta^6$ -bound to chromium. This point will be addressed in more detail below. For ferrocene, the CBS(T) value of  $-3.00 \text{ kcal mol}^{-1}$  is also more negative than the value in free benzene, albeit to a lesser extent. As is well documented for  $\pi$ -stacked complexes, MP2 overestimates binding by around 50 %, with the MP2 basis set limit as much as  $2 \text{ kcal mol}^{-1}$  greater than the best estimate. In this case, the contributions to binding from triple excitations are rather large, 0.86 and  $0.73 \text{ kcal mol}^{-1}$ , clearly demonstrating that such excitations cannot be neglected. DF-LMP2 is again close to DF-MP2 in strongly overestimating binding, whereas SCS, SCSN and SCS(MI) scaling yield good agreement with CBS(T) values. In contrast, SCSC scaling values lead to significant overestimation of binding, suggesting they are less appropriate for these complexes. All DFT methods yield stable complexes, unlike HF, but agreement with CBS(T) is rather poor, with errors of between 1 and  $2 \text{ kcal mol}^{-1}$ , the former error being more typical of the behaviour previously reported.<sup>[9]</sup> For these PD complexes, the M06-2X functional appears to best reproduce CBS(T) data, with errors of approximately  $1 \text{ kcal mol}^{-1}$ .

As well as the PD form, T-shaped complexes can be formed between  $\text{Cr}(\text{C}_6\text{H}_6)(\text{CO})_3$  and  $\text{C}_6\text{H}_6$  with the metal complex as either the donor or the acceptor of a hydrogen bond, as shown in Figure 1. In the former, the threefold symmetry of the metal complex means that two distinct complexes must be considered, donating through C–H that is either in the eclipsed or staggered position relative to a carbonyl, which we denote T2a and T2b. Data from DF-LMP2 scans of each of these are shown in Figure 4. As in previous scans, SCSN values are bracketed by DF-LMP2 and SCS in all cases. These curves, with all three methods, clearly show that  $\text{Cr}(\text{C}_6\text{H}_6)(\text{CO})_3$  is a much better hydrogen-bond donor to benzene than it is a hydrogen-bond acceptor from benzene. Complex T1 reaches maximum stabilisation of slightly more than  $-2 \text{ kcal mol}^{-1}$ , whereas complexes T2a

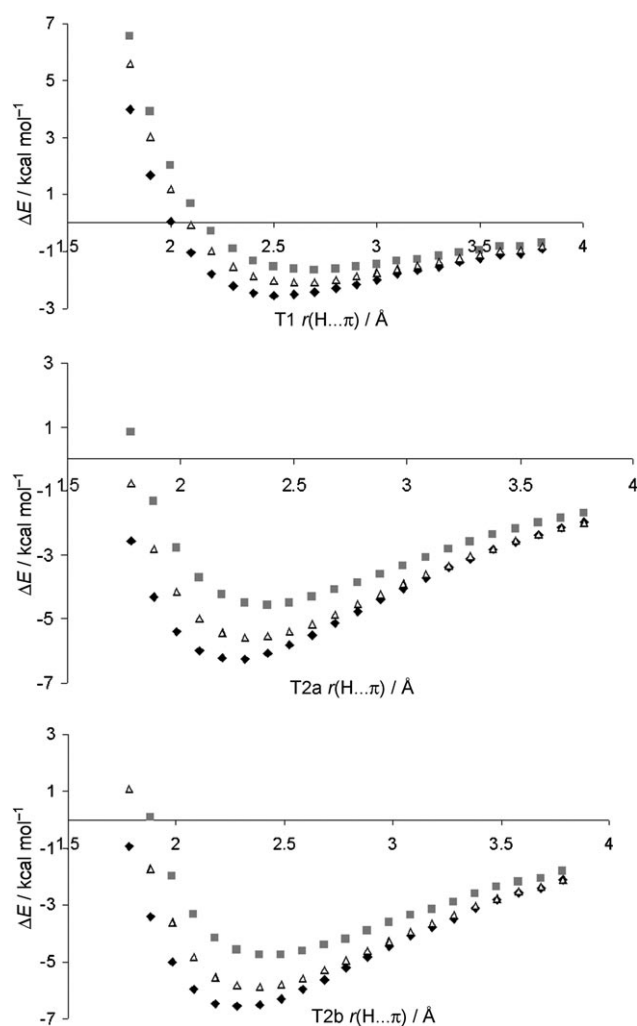


Figure 4. Scan of T-shaped complexes of  $\text{Cr}(\text{C}_6\text{H}_6)(\text{CO})_3$  with  $\text{C}_6\text{H}_6$  (♦ = DF-LMP2, ■ = SCS and △ = SCSN).

and T2b have maximum stabilisations of almost  $-6 \text{ kcal mol}^{-1}$ . Moreover, complex T2b (with the C–H donor staggered between the CO ligands) is more stable than complex T2a by approximately  $0.3 \text{ kcal mol}^{-1}$ .

Table 2 reports CBS(T) and related data for the minima on the SCSN curves for T1 and T2b complexes. This confirms the initial finding that  $\text{Cr}(\text{C}_6\text{H}_6)(\text{CO})_3$  is a significantly stronger hydrogen-bond donor than hydrogen-bond acceptor in such T-shaped complexes, the two forms differing by as much as  $4 \text{ kcal mol}^{-1}$ . The T2b complex is more than  $1.5 \text{ kcal mol}^{-1}$  more stable than the PD one, unlike the free benzene dimer in which stacked and T-shaped forms are almost isoenergetic. Thus, the presence of the transition metal significantly alters the propensity of benzene to form intermolecular interactions. Once again, DF-MP2 and DF-LMP2 methods substantially overestimate the strength of binding, whereas SCSN, SCS(MI) and SCSC scaling of the latter reproduces the CBS(T) data with impressive accuracy. The importance of dispersion contributions to the bind-

ing energy in these C–H... $\pi$  complexes is demonstrated by the lack of binding at the HF level, whereas both DFT methods tested perform adequately with errors in the region of  $1 \text{ kcal mol}^{-1}$ .

The higher symmetry of ferrocene means that only two T-shaped complexes between  $\text{Fe}(\text{C}_5\text{H}_5)_2$  and  $\text{C}_6\text{H}_6$  were scanned by using DF-LMP2 methods, with the results shown

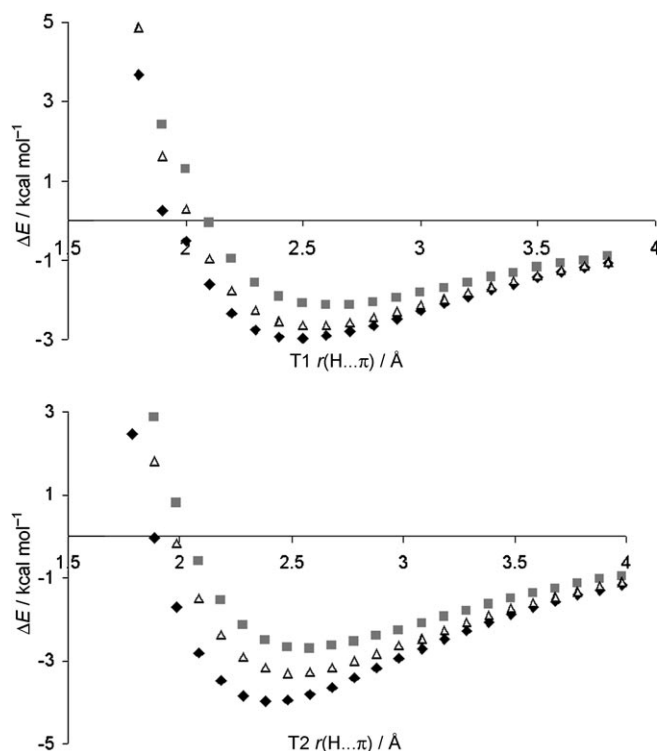


Figure 5. Scan of T-shaped complexes of  $\text{Fe}(\text{C}_5\text{H}_5)_2$  with  $\text{C}_6\text{H}_6$  in T1 and T2 orientations (♦ = DF-LMP2, ■ = SCS and △ = SCSN).

in Figure 5. Once again, the SCSN curves are bracketed by unscaled DF-LMP2 and SCS ones. The difference between T1 and T2 forms here is less marked, but the pattern is the same: ferrocene is a better hydrogen-bond donor to benzene than it is a hydrogen-bond acceptor from benzene. At the minima of the SCSN curves (2.5 and  $4.8 \text{ Å}$ ), the interaction energies are  $-2.65$  and  $-3.28 \text{ kcal mol}^{-1}$ , respectively. The CBS(T) data in Table 2 confirm this, showing that the T2 form is  $0.7 \text{ kcal mol}^{-1}$  more stable than the T1 form. The former has similar interaction energy to the T-shaped benzene dimer (binding energy of  $-2.68 \text{ kcal mol}^{-1}$ ), indicating that the coordinated cyclopentadienyl ring in ferrocene has similar hydrogen-bond acceptor properties to benzene, but is a slightly stronger hydrogen-bond donor than free benzene. In both cases, MP2 overestimates the strength of interaction, whereas SCSN, SCS(MI) and SCSC are in good agreement with CBS(T) data. All three DFT methods give reasonable agreement with the best estimate, with BHandH apparently performing well here.



The data presented above indicates that a benzene ring coordinated to  $\text{Cr}(\text{CO})_3$  is a slightly weaker hydrogen-bond acceptor than free benzene, but that such a ring is a rather strong hydrogen-bond donor and forms significantly stronger  $\pi$ -stacking interactions than free benzene. The origins of this behaviour were probed further by analysing the properties of  $\text{Cr}(\text{C}_6\text{H}_6)(\text{CO})_3$  itself. NBO analysis by using BP86/6-31+G(d,p) indicates strong donation from the  $\pi$  system of benzene into formally empty Cr d orbitals, balanced by back-donation from filled metal d orbitals into  $\pi^*$  orbitals on benzene. The former dominates, resulting in a net charge on benzene in the complex of +0.12 e. Closer inspection indicates that this net positive charge on benzene is located entirely on the hydrogen atoms: NBO charges on the hydrogen atoms average +0.298 in the coordinated benzene, compared with +0.262 in free benzene, whereas charges on the carbon atoms are very slightly more negative in the complex than in benzene. Second-order perturbative NBO analysis data shows that stabilisation by donation from benzene  $\pi$  orbitals into chromium d orbitals is significantly stronger (401.90 kcal mol<sup>-1</sup>) than that from back-donation from d into  $\pi^*$  orbitals (132.25 kcal mol<sup>-1</sup>).

In ferrocene the charge on iron is +0.399 and -0.200 on each ring, indicating significant deviation from the formal charges of +2 and -1, but retaining the overall pattern of electron distribution. The stabilisation energy associated with donation from each of the cyclopentadiene units to iron is 484.46 kcal mol<sup>-1</sup>, whereas the back-donation from iron to the cyclopentadiene units is much weaker in comparison at 85.32 kcal mol<sup>-1</sup>.

These patterns of electron distribution are reflected in the molecular electrostatic potential generated by the metal complexes, as shown in Figure 6, in which the only significantly positive values are located close to aromatic hydrogen atoms. The corresponding values for free benzene (not shown) exhibit less pronounced maxima associated with C-H bonds (maxima +0.025 a.u. in benzene, +0.044 a.u. in

$\text{Cr}(\text{C}_6\text{H}_6)(\text{CO})_3$  and +0.029 in ferrocene) but also a minimum over the ring centroid, a feature that is absent in the chromium complex but evident in ferrocene. Thus, it seems evident that net donation of electrons from benzene to Cr, and the concomitant changes in electron density around benzene, lead to the reduced hydrogen-bond accepting and increased hydrogen-bond donating ability of the coordinated benzene. This effect is less pronounced in ferrocene because net negative charge of each ring is retained.

These changes do not, at first sight, explain the large increase in  $\pi$ -stacking interaction energy shown in Table 2 and Figure 3 for the chromium complex, because net donation from the  $\pi$  system of benzene should lead to reduced dispersion interactions. However, these changes do contribute to the increased binding in the PD complex: in the free benzene dimer at the same separation, the BSSE-corrected HF/AVTZ\* interaction energy is +4.13 kcal mol<sup>-1</sup>, whereas in Table 2 we find +3.11 kcal mol<sup>-1</sup>. This difference of 1.02 kcal mol<sup>-1</sup> is a substantial fraction (64%) of the overall difference between free and chromium-bound benzene dimers, indicating that increased electrostatic attraction and/or reduced exchange-repulsion play a part in the increased binding of this complex.

Local correlation methods allow us to decompose correlation contributions to the binding energy from individual orbitals and/or atoms, functional groups or whole molecules. Comparison of such decomposition for the PD complex with the analogous benzene dimer (Table 3) from

Table 3. Intermolecular correlation energies in PD complexes [kcal mol<sup>-1</sup>].

	$\text{Cr}(\text{C}_6\text{H}_6)(\text{CO})_3 \cdots \text{C}_6\text{H}_6$	Benzene dimer
total	-8.99	-8.43
dispersion	-6.73	-6.27
ionic	-2.30	-2.17
$\pi \cdots \pi$	-2.55	-2.96
Cr $\cdots$ benzene	-0.87	-

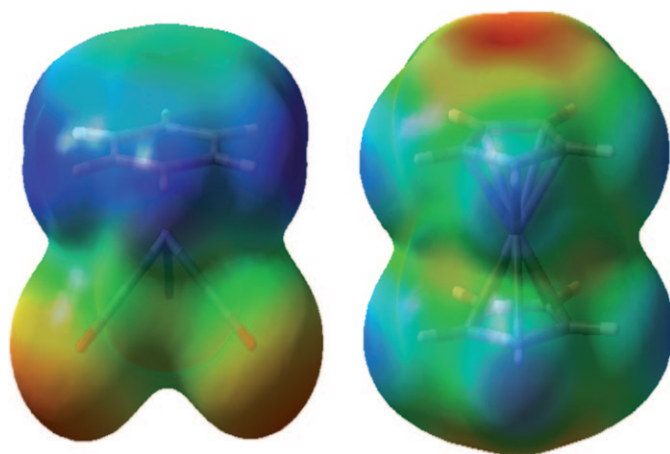


Figure 6. Molecular electrostatic potential around  $\text{Cr}(\text{C}_6\text{H}_6)(\text{CO})_3$  and ferrocene at the BP86/6-31+G(d,p) level, projected onto the 0.001 au isodensity contour. Blue represents positive MEP and red represents negative MEP.

DF-LMP2/AVTZ\* confirms the increased intermolecular correlation in the chromium complex. Coupled with the increased binding at the HF level, this accounts for essentially all the increased binding of the metal complex. Table 3 also indicates that dispersion interactions dominate this intermolecular correlation, but that ionic terms (double excitations from the occupied orbitals of one monomer to the virtual orbitals of the other) are substantial in both cases. Isolating just the interactions between  $\pi$  orbitals in each monomer (by using Löwdin charges as the criteria) reveals that the withdrawal of electron density from benzene by complexation to Cr does indeed reduce the strength of the stacking interaction. However, this is more than offset by the interactions of orbitals predominantly based on Cr with the stacked benzene, which at -0.87 kcal mol<sup>-1</sup> are surprisingly strongly stabilising. The bulk (-0.55 kcal mol<sup>-1</sup>, 63%) of these Cr interactions are with the  $\pi$  orbitals of benzene, with the remainder made up from individually small (-0.02 to

−0.05 kcal mol<sup>−1</sup>) but cumulatively significant contributions from C–C and C–H  $\sigma$ -bonding orbitals.

Rigid scans by using BHandH were also carried out on the ferrocene and Cr(C<sub>6</sub>H<sub>6</sub>)(CO)<sub>3</sub> complexes with methane and the PD, T1 and T2 conformations of benzene. Data from these scans is summarised in Table 4, along with analo-

Table 4. Equilibrium distances [Å] and interaction energies [kcal mol<sup>−1</sup>] of Cr(C<sub>6</sub>H<sub>6</sub>)(CO)<sub>3</sub> and Fe(C<sub>5</sub>H<sub>5</sub>)<sub>2</sub> at equilibrium distances.

	DF-LMP2		SCSN		BHandH	
	<i>r</i> <sub>eq</sub>	$\Delta E$	<i>r</i> <sub>eq</sub>	$\Delta E$	<i>r</i> <sub>eq</sub>	$\Delta E$
Cr(C <sub>6</sub> H <sub>6</sub> )(CO) <sub>3</sub>						
CH <sub>4</sub>	2.80	−1.38	2.90	−1.11	2.60	−1.60
PD	3.30	−5.80	3.50	−4.35	3.40	−3.00
T1	2.50	−2.53	2.60	−2.08	2.50	−2.06
T2b	4.80	−6.55	4.90	−5.89	4.80	−6.27
Fe(C <sub>5</sub> H <sub>5</sub> ) <sub>2</sub>						
CH <sub>4</sub>	2.80	−1.44	2.80	−1.23	2.50	−1.97
PD	3.30	−4.14	3.50	−2.71	3.40	−1.67
T1	2.50	−2.97	2.50	−2.65	2.40	−3.02
T2	4.70	−3.95	4.80	−3.28	4.70	−3.23

gous data from DF-LMP2 and SCSN for comparison. These results show that the curves have minima at similar equilibrium distances to DF-LMP2 and/or SCSN, whereas interaction energies at these minima follow the same trends as seen in Table 2. For both CH<sub>4</sub> complexes, interaction energies are overestimated and hence separation is underestimated (relative to SCSN). For both PD complexes, BHandH scans have consistently reduced the interaction energy, and run almost parallel to the SCSN curves, such that rather similar minima have been found. Performance is best for the T-shaped complexes, for which BHandH and SCSN curves are close across all separations. Table 4 indicates that, in general, BHandH is as successful in locating minimum energy geometry as is unscaled MP2, and hence could be an efficient method for optimising larger, more complex systems in which the rigid scan technique would be unsuitable. This prompted us to explore this as an approach to full geometry optimisation. Previous work shows that this approach gives reasonable approximations to high-level optimised geometries, even in cases in which interaction energies are significantly in error.<sup>[40]</sup> We, therefore, performed unconstrained geometry optimisations for four complexes of Cr(C<sub>6</sub>H<sub>6</sub>)(CO)<sub>3</sub>, and the resulting structures are shown in Figure 7, along with selected geometrical parameters.

The methane complex barely differs from the minimum of the rigid scan, retaining approximate C<sub>3v</sub> symmetry with a single C–H bond pointing towards the  $\pi$  system at a distance of 2.50 Å from the centroid of the ring. Similarly, the PD complex retains the essential features from Figure 3, with parallel benzene moieties at 3.6 Å apart. In this case, however, there is little or no barrier to conversion to the T2b orientation: default optimisation options result in spontaneous movement to the T-shaped form, whereas calculation of initial force constants from harmonic frequencies, or

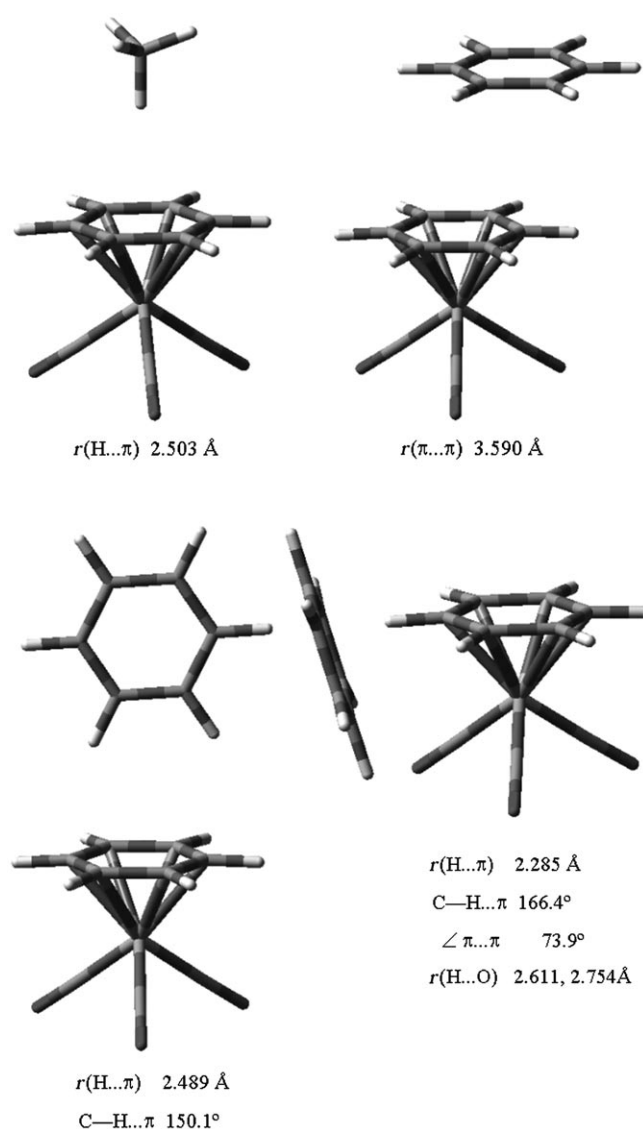


Figure 7. BHandH/6-31+G(d,p) optimised geometries.

optimisation in Cartesian rather than internal coordinates, locates the form shown in Figure 7 as a local minimum.

Significant differences from the results of rigid scans are observed on optimisation of both T1 and T2b orientations. In the former, the C–H donor no longer points directly towards the centroid of the acceptor, but instead assumes an off-centre position. This has been observed previously for the free benzene dimer, in which it was found to be approximately 0.2 kcal mol<sup>−1</sup> more stable than the higher-symmetry T-shaped form. Similarly, the T2b form does not retain the perpendicular orientation employed for Figure 4, adopting an orientation that brings two hydrogen atoms of benzene into reasonably close contact with one of the carbonyl oxygen atoms. Atoms-in-molecules analysis (not shown) confirms the presence of a C–H $\cdots$ O interaction as well as the expected C–H $\cdots\pi$  hydrogen bond in this orientation.

Even with the relatively efficient DF-LMP2 or SCSN methods, full optimisation requires more CPU resources

than are currently available to us, making identification of such geometrical subtleties by any other means than DFT a difficult and laborious task. It may be that other DFT approaches specifically designed to better describe non-covalent interactions will be preferable to BHandH in this regard, but in the absence of benchmark geometry for proper comparison this cannot be determined at present. In any case, detailed comparison of DFT methods is not the main goal of this work.

## Conclusion

Benchmark ab initio data determine the strength of interaction of chromium benzene tricarbonyl and ferrocene with methane and benzene, the latter in various orientations to give C–H $\cdots\pi$  and  $\pi\cdots\pi$ -stacking interactions. Compared with benzene, both metal complexes are slightly weaker hydrogen-bond acceptors to both methane and benzene, but are significantly stronger hydrogen-bond donors to the  $\pi$  system of benzene. The most strongly bound complex, that of Cr(C<sub>6</sub>H<sub>6</sub>)(CO)<sub>3</sub> donating a C–H $\cdots\pi$  hydrogen bond to benzene, has an interaction energy of  $-5.85$  kcal mol<sup>-1</sup>, more than twice the value of  $-2.68$  kcal mol<sup>-1</sup> previously found for the T-shaped benzene dimer. The PD,  $\pi$ -stacked complex between the chromium compound and benzene is also much more stable than the equivalent benzene dimer.

This benchmark data allows us to test the performance of less accurate but more efficient MP2 and DFT methods. As in non-metal cases, standard MP2 methods strongly overestimate interaction energies. This behaviour can be remedied by use of SCS, with two variants of this approach designed specifically for non-covalent interactions showing promise in this regard. A third approach, SCSC, performs well for CH<sub>4</sub> and T-shaped complexes, but less well for PD ones. When combined with density fitting and local correlation methods, the DF-SCSN-LMP2 method is an efficient and accurate method for determining interaction energies, allowing potential energy surface scans for intermolecular coordinates.

The origins of the observed trends in interaction energy are explored in more detail, and can largely be traced to the net transfer of electron density from the aromatic ligand into metal d orbitals. This apparently has a larger effect on aromatic hydrogen electron populations, thus promoting the hydrogen-bond donor capacity of these ligands. The enhanced  $\pi\cdots\pi$  stacking, most evident in the chromium complex, can be traced partially to the same redistribution of electrons and partially to additional dispersion interactions with the metal centre. Finally, the utility of an efficient DFT method for geometry optimisation is demonstrated, and the importance of performing full optimisation rather than one-dimensional scans is discussed.

## Acknowledgements

The authors are grateful to the Advanced Research Computing (ARCCA) facility at Cardiff University and the EPSRC National Service for Computational Chemistry Software (NSCCS) for the use of computing resources.

- [1] E. A. Meyer, R. K. Castellano, F. Diederich, *Angew. Chem.* **2003**, *115*, 1244; *Angew. Chem. Int. Ed.* **2003**, *42*, 1210, and references therein.
- [2] J. Šponer, K. E. Riley, P. Hobza, *Phys. Chem. Chem. Phys.* **2008**, *10*, 2595.
- [3] S. Tsuzuki, A. Fujii, *Phys. Chem. Chem. Phys.* **2008**, *10*, 2584.
- [4] W. Wang, M. Pitoňák, P. Hobza, *ChemPhysChem* **2007**, *8*, 2107.
- [5] a) S. Tsuzuki, K. Honda, T. Uchimaru, M. Mikami, K. Tanabe, *J. Am. Chem. Soc.* **2002**, *124*, 104; b) M. O. Sinnokrot, C. D. Sherrill, *J. Phys. Chem. A* **2006**, *110*, 10656; c) J. G. Hill, J. A. Platts, H.-J. Werner, *Phys. Chem. Chem. Phys.* **2006**, *8*, 4072.
- [6] For examples, see: a) P. Hobza, H. L. Selzle, E. W. Schlag, *J. Phys. Chem. B* **1996**, *100*, 18790; b) P. Jurecka, P. Hobza, *Chem. Phys. Lett.* **2002**, *365*, 89.
- [7] a) C. A. Morgado, P. Jurečka, D. Svozil, P. Hobza, J. Šponer, *J. Chem. Theory Comput.* **2009**, *5*, 1524; b) P. Dedíková, M. Pitoňák, P. Neogrády, I. Černušák, M. Urban, *J. Phys. Chem. A* **2008**, *112*, 7115; c) A. D. Boese, J. M. L. Martin, W. Klopper, *J. Phys. Chem. A* **2007**, *111*, 11122; d) Y. Zhao, D. G. Truhlar, *J. Phys. Chem. A* **2005**, *109*, 6624; e) P. Jurecka, P. Hobza, *J. Am. Chem. Soc.* **2003**, *125*, 15608.
- [8] a) E. R. Johnson, R. A. Wolkow, G. A. DiLabio, *Chem. Phys. Lett.* **2004**, *394*, 334; b) J. Cerný, P. Hobza, *Phys. Chem. Chem. Phys.* **2005**, *7*, 1624.
- [9] a) M. P. Waller, A. Robertazzi, J. A. Platts, D. E. Hibbs, P. A. Williams, *J. Comput. Chem.* **2006**, *27*, 491; b) Y. Zhao, D. G. Truhlar, *J. Chem. Theory Comput.* **2008**, *4*, 1849; c) Y. Zhao, D. G. Truhlar, *Theor. Chem. Acc.* **2008**, *120*, 215.
- [10] a) S. Grimme, *J. Comput. Chem.* **2004**, *25*, 1463; b) J. Antony, S. Grimme, *Phys. Chem. Chem. Phys.* **2006**, *8*, 5287; c) P. Jurečka, J. Cerný, P. Hobza, D. R. Salahub, *J. Comput. Chem.* **2007**, *28*, 555; d) O. A. von Lilienfeld, I. Tavernelli, U. Rothlisberger, D. Sebastiani, *Phys. Rev. Lett.* **2004**, *93*, 153004.
- [11] S. Grimme, *J. Chem. Phys.* **2003**, *118*–119 9095.
- [12] M. Korth, A. Lüchow, S. Grimme, *J. Phys. Chem. A* **2008**, *112*, 2104.
- [13] a) O. Marchetti, H.-J. Werner, *Phys. Chem. Chem. Phys.* **2008**, *10*, 3400; b) J. R. Lane, H. G. Kjaergaard, *J. Chem. Phys.* **2009**, *131*, 034307.
- [14] a) J. Huang, G. L. Rempel, *Progr. Polymer Sci.* **1995**, *20*, 459; b) C. Janiak, *Coord. Chem. Rev.* **2006**, *250*, 66.
- [15] a) S. Aldridge, C. Bresner, I. A. Fallis, S. J. Coles, M. B. Hursthouse, *Chem. Commun.* **2002**, 740; b) M. Nakayama, T. Ihara, K. Nakano, M. Maeda, *Talanta* **2002**, *56*, 857.
- [16] a) B. M. Zeglis, V. C. Pierre, J. K. Barton, *Chem. Commun.* **2007**, 4565; b) F. R. Keene, J. A. Smith, J. G. Collins, *Coord. Chem. Rev.* **2009**, *253*, 2021.
- [17] a) A. F. A. Peacock, P. J. Sadler, *Chem. Asian J.* **2008**, *3*, 1890; b) S. J. Dougan, P. J. Sadler, *Chimia* **2007**, *61*, 704.
- [18] H.-J. Werner, P. J. Knowles, R. Lindh, F. R. Manby, M. Schütz, P. Celani, T. Korona, A. Mitrushenkov, G. Rauhut, T. B. Adler, R. D. Amos, A. Bernhardsson, A. Berning, D. L. Cooper, M. J. O. Deegan, A. J. Dobyn, F. Eckert, E. Goll, C. Hampel, G. Hetzer, T. Hrenar, G. Knizia, C. Köppl, Y. Liu, A. W. Lloyd, R. A. Mata, A. J. May, S. J. McNicholas, M. E. M. Meyer, M. E. Mura, A. Nicklass, P. Palmieri, K. Pflüger, R. Pitzer, M. Reiher, U. Schumann, H. Stoll, A. J. Stone, R. Tarroni, T. Thorsteinsson, M. Wang, A. Wolf, MOLPRO, version 2008.2, a package of ab initio programs, see <http://www.molpro.net>.
- [19] a) T. H. Dunning Jr., *J. Chem. Phys.* **1989**, *90*, 1007; b) R. A. Kendall, T. H. Dunning Jr., R. Harrison, *J. Chem. Phys.* **1992**, *96*, 6796; c) N. B. Balabanov, K. A. Peterson, *J. Chem. Phys.* **2005**, *123*, 064107.



- [20] a) R. Polly, H.-J. Werner, F. R. Manby, P. J. Knowles, *Mol. Phys.* **2004**, *102*, 2311; b) H.-J. Werner, F. R. Manby, P. J. Knowles, *J. Chem. Phys.* **2003**, *118*, 8149.
- [21] a) F. Weigend, A. Köhn, C. Hättig, *J. Chem. Phys.* **2002**, *116*, 3175; b) J. G. Hill, J. A. Platts, *J. Chem. Phys.* **2008**, *128*, 044104.
- [22] F. Weigend, *J. Comput. Chem.* **2008**, *29*, 167.
- [23] T. Helgaker, W. Klopper, H. Koch, J. Noga, *J. Chem. Phys.* **1997**, *106*, 9639.
- [24] S. F. Boys, F. Bernardi, *Mol. Phys.* **1970**, *19*, 553.
- [25] a) P. Pulay, *Chem. Phys. Lett.* **1983**, *100*, 151; b) S. Saebø, P. Pulay, *Annu. Rev. Phys. Chem.* **1993**, *44*, 213; c) C. Hampel, H.-J. Werner, *J. Chem. Phys.* **1996**, *104*, 6286.
- [26] J. G. Hill, J. A. Platts, H.-J. Werner, *Phys. Chem. Chem. Phys.* **2006**, *8*, 4072.
- [27] J. Pipek, P. G. Mezey, *J. Chem. Phys.* **1989**, *90*, 4916.
- [28] J. W. Boughton, P. J. Pulay, *J. Comput. Chem.* **1993**, *14*, 736.
- [29] M. Schütz, G. Rauhut, H.-J. Werner, *J. Phys. Chem. A* **1998**, *102*, 5997.
- [30] S. Grimme, *Chem. Eur. J.* **2004**, *10*, 3423.
- [31] J. G. Hill, J. A. Platts, *J. Chem. Theory Comput.* **2007**, *3*, 80.
- [32] R. A. Distasio M. Head-Gordon, *Mol. Phys.* **2007**, *105*, 1073.
- [33] Y. Zhao, D. G. Truhlar, *J. Chem. Theory Comput.* **2009**, *5*, 324.
- [34] Gaussian 09, Revision A.02, M. J. Frisch, G. W. Trucks, H. B. Schlegel, G. E. Scuseria, M. A. Robb, J. R. Cheeseman, G. Scalmani, V. Barone, B. Mennucci, G. A. Petersson, H. Nakatsuji, M. Caricato, X. Li, H. P. Hratchian, A. F. Izmaylov, J. Bloino, G. Zheng, J. L. Sonnenberg, M. Hada, M. Ehara, K. Toyota, R. Fukuda, J. Hasegawa, M. Ishida, T. Nakajima, Y. Honda, O. Kitao, H. Nakai, T. Vreven, J. A. Montgomery, Jr., J. E. Peralta, F. Ogliaro, M. Bearpark, J. J. Heyd, E. Brothers, K. N. Kudin, V. N. Staroverov, R. Kobayashi, J. Normand, K. Raghavachari, A. Rendell, J. C. Burant, S. S. Iyengar, J. Tomasi, M. Cossi, N. Rega, J. M. Millam, M. Klene, J. E. Knox, J. B. Cross, V. Bakken, C. Adamo, J. Jaramillo, R. Gomperts, R. E. Stratmann, O. Yazyev, A. J. Austin, R. Cammi, C. Pomelli, J. W. Ochterski, R. L. Martin, K. Morokuma, V. G. Zakrzewski, G. A. Voth, P. Salvador, J. J. Dannenberg, S. Dapprich, A. D. Daniels, O. Farkas, J. B. Foresman, J. V. Ortiz, J. Cioslowski, D. J. Fox, Gaussian, Inc., Wallingford CT, **2009**.
- [35] a) W. J. Hehre, R. Ditchfield, J. A. Pople, *J. Chem. Phys.* **1972**, *56*, 2257; b) M. J. Frisch, J. A. Pople, J. S. Binkley, *J. Chem. Phys.* **1984**, *80*, 3265.
- [36] a) A. D. Becke, *Phys. Rev. A* **1998**, *38*, 3098; b) J. P. Perdew, *Phys. Rev. B* **1986**, *33*, 8822.
- [37] A. E. Reed, L. A. Curtiss, F. Weinhold, *Chem. Rev.* **1988**, *88*, 899.
- [38] Y. Wang, K. Angermund, R. Goddard, C. Kruger, *J. Am. Chem. Soc.* **1987**, *109*, 587.
- [39] a) A. Haaland, J. Nilsson, *Acta Chem. Scand.* **1968**, *22*, 2653; b) S. Coriani, A. Haaland, T. Helgaker, P. Jørgensen, *ChemPhysChem* **2006**, *7*, 245.
- [40] K. Gkionis, J. G. Hill, S. P. Oldfield, J. A. Platts, *J. Mol. Model.* **2009**, *15*, 1051.

Received: October 12, 2009  
Published online: April 1, 2010